Geomorphology 180–181 (2013) 24–32

Contents lists available at SciVerse ScienceDirect

Geomorphology

journal homepage: www.elsevier.com/locate/geomorph

Numerical simulation of the evolution and propagation of aeolian dune fields toward a desert–oasis zone

Tian-Li Bo *, Xiao-Jing Zheng

Key Laboratory of Mechanics on Western Disaster and Environment, Lanzhou University, Lanzhou, 730000, China
Department of Mechanics, Lanzhou University, Lanzhou, 730000, China

ARTICLE INFO

Article history:
Received 23 March 2012
Received in revised form 1 September 2012
Accepted 12 September 2012
Available online 19 September 2012

Keywords:
Desert–oasis transitional zone
Propagation speed
Edge of desertified land
Vegetation coverage
Straw checkerboard area

ABSTRACT

In this study, the evolution and propagation of aeolian dune fields toward a desert–oasis transitional zone are numerically investigated through considering the spatial variation of wind speed and the influence of vegetation on sand erosion and transportation etc. The propagation speed at the edge of desertified land and the influence of a straw checkerboard are quantitatively analyzed. Results show that evolution time, wind speed and sand diameter have obvious impacts on the propagation of desert and desertified land. A formula describing the propagation speed of desertified land with respect to wind speed and vegetation coverage is given. In addition, when considering the effects of straw checkerboards, the propagation speed of the downwind desertified land is found to be related to the length of and distance from the checkerboard area.

1. Introduction

As a typical geomorphologic feature in arid and semi-arid areas, dune fields are often accompanied by oases adjacent to the edge of deserts (Wang et al., 2006). Due to the influence of human activities, such as overgrazing and excessive land reclamation, oases in arid and semi-arid areas are gradually degrading into desert–oasis transitional zones with the development and spread of desertification (Li et al., 2001; Fu and Lu, 2006; Chen et al., 2008). The desert–oasis transitional zone plays an important role in the ecological system of arid and semi-arid areas, which maintains the sustainable development of local economy and internal stability of agriculture, helps to fix mobile sand dunes, and protects the oasis from wind-blown sand damage. In addition, the mobility of the dune field is an important index for reflecting global climate change and desertification (Thomas et al., 2005; Yizhaq et al., 2009), which therefore becomes an important issue in environmental science.

Minqin, located at 103.09°E, 38.62°N, is an oasis wedging itself between the 5th and 6th largest deserts in China, the Badain Jaran Desert and Tengger Desert respectively (Wang and Cui, 2004), and prevents the two deserts from merging, as shown in Fig. 1. The area of desert and desertified land in Minqin has already reached up to 14,450 km^2, taking up 91% of the total area, and the edge of desertified land is approaching the oasis at a speed of 3–4 m per year, which makes the county one of the four most important sand (dust) storm sources in China (Zheng, 2009). Since a decade ago, desertification monitoring schemes and sand control measures, including setting sand fences and straw checkerboards, have been implemented to maintain the oasis from the invasion of aeolian dunes at the edge of deserts and desertified lands.

Due to the extremely large spatial and temporal scales involved in the evolution and propagation of aeolian dune fields, existing observational facilities and schemes have not achieved a panoramic survey of the whole process of dune fields in the desert–oasis transitional zone. However, theoretical modeling and numerical simulations have provided important insights to the evolution of dune fields in desert–oasis transitional zones (Nishimori and Ouchi, 1993; Werner, 1995; Momiji et al., 2000; Sauermann et al., 2001; Schwammle and Herrmann, 2003; Parteli et al., 2007; Narteau et al., 2009).

It has been argued that vegetation coverage has an important impact on the morphology of aeolian dunes (Wasson and Hyde, 1983; Rubin and Hunter, 1987), which therefore has an influence on the evolution of dunes and dune fields. In this field, the most significant issue is dunes' stability and the barchan–parabolic dune transition process. Parabolic dunes have long arms that point upwind and noses that point downwind. They arise commonly as a result of the stabilization of barchan dunes by vegetation (Hack, 1941; Gaylord and Stetler, 1994; Muckersie and Shepherd, 1995; Anthonsen et al., 1996; Tsoar and Blumberg, 2002; Yizhaq et al., 2007). The barchan–parabolic dune transition process has been observed on individual dunes where changes in climate or land-use have introduced vegetation to a dune surface, the reversal of parabolic to barchan shape upon the removal of vegetation has also been observed, and barchan–

* Corresponding author at: Key Laboratory of Mechanics on Western Disaster and Environment, Lanzhou University, Lanzhou, 730000, China. Tel.: +86 931 8915336; fax: +86 931 8915336.
E-mail address: btl@lzu.edu.cn (T.-L. Bo).

0169-555X/$ – see front matter
http://dx.doi.org/10.1016/j.geomorph.2012.09.002

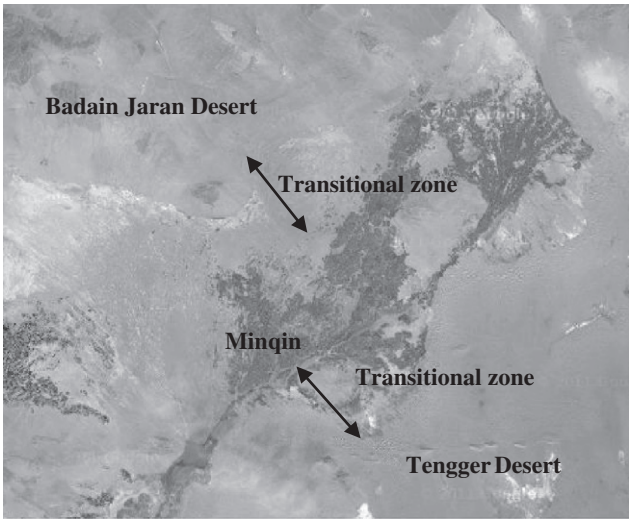

Fig. 1. The desert–oasis transitional zone of Minqin, China.

parabolic dune pattern transition from vegetation stability threshold has been proposed (Hack, 1941; Anthonsen et al., 1996; Tsoar and Blumberg, 2002; Wolfe and Hugenholtz, 2009; Reitz et al., 2010).

Quantitative simulation is another important method with which to study this phenomenon. Cellular automaton and continuum models have simulated parabolic dune formation and furthered our quantitative knowledge of the barchan–parabolic transition. The cellular model of Nishimori and Tanaka (2001) partially succeeded in capturing the transition. In their simulation, barchan dunes temporarily gave rise to parabolic forms that were unstable. A cellular model by Nield and Baas (2008), which simulated the development of parabolic dunes from blowouts rather than barchans, produced stable parabolic dunes by incorporating two plant species requiring different growth environments. The continuum model that simulates the barchan–parabolic transition is that of Durán et al. (Durán and Herrmann, 2006; Luna et al., 2009), which uses a set of differential equations relating the relative timescales of vegetation growth and dune surface erosion/deposition. Their simulation succeeds in qualitatively reproducing the transition process and predicts a critical ratio θ_c of total surface change to vegetation growth rate, above which a barchan is stable and below which vegetation takes hold and a parabolic dune forms. Durán et al. (2008) compared the vegetation cover on a dune blowout in Brazil to a simulated blowout with an arbitrarily selected fixation index and find qualitative similarity. In addition, Luna et al. (2011) achieved the quantitative simulation of coastal dune field which has a length of 512 m transverse to the wind and 1024 m in the wind direction using the continuum model; in their paper, they discussed the influence of sand influx, the width of the vegetation-free backshore, maximum vegetation height, vegetation growth and wind shear velocities on dune field morphology.

From above, existing simulations can be found on the impact of vegetation on the dune or dune field which focus on dune field morphology, the dune stability, and the barchan–parabolic transition process, but there has been little focus on the impact of vegetation on the propagation of the edge of desertified land and the study of the evolution of dune field in desert–oasis transitional zone. Only Yizhaq et al. (2007) proposed a model for dune vegetation cover driven by wind power that exhibited bi-stability and hysteresis with respect to the wind power. However, the establishment of their model was not based on the simulation of the dune field.

Recently, Zheng and co-workers (Zheng, 2009; Zheng et al., 2009; Bo and Zheng, 2011a, 2011b) developed a scale-coupled model of dune fields (CSCDUNE), in which the 'sand body element' concept is proposed to bridge the multi-scales involved in the underlying processes, ranging from the motion of sand particles to the evolution of dunes as the representative element used to analyze the spallation in solids (Aidun et al., 1999). The size of the eroded 'sand body element' in the model is determined by the basic processes of wind-blown sand movements, including erosion, deposition, wind-blown sand flux and the wind intensity at various locations. The motion of the eroded 'sand body element' is determined by the transportation and deposition of the wind-blown sand flux, as well as the 'avalanche' behavior of sand particles (Zheng, 2009; Zheng et al., 2009; Bo and Zheng, 2011a, 2011b). The relationship between the average saltation length of sand particles and the transportation length of the eroded 'sand body element' was established. Consequently, a correspondence between simulation results and the actual evolution of a dune field is obtained in both the spatial and temporal scales. The temporal and spatial scales in the model which have a span of 8~9 orders of magnitude, from the motion of a single particle (the size and saltation time of sand particles are 10^{-4} m and 10^{-2}~10^{-1} s, respectively) to the formation and evolution of the whole dune field (the size and evolution time of dune field are 10^{0}~10^{4} m and 10^{4}~10^{8} s, respectively), can be established. It has shown that the morphology (the relation between width, length and height) and change law (the relation between average dune height and sand supply, and the relation between dune speed and dune height) of a dune field obtained by the CSCDUNE scheme are consistent with observation results.

In this study, using the treatment of vegetation in the cellular model (Nishimori and Tanaka, 2001) and the continuum model of sand dunes (Durán and Herrmann, 2006) for reference, we conduct quantitative simulations of the formation and evolution of dune fields in the desert–oasis transitional zone, through considering the spatial variation of wind speed, the influence of vegetation cover on sand erosion and transportation of sand particles in CSCDUNE. Further, the variation laws of the propagation speed at the edge of the desert and desertified land with local wind speed, sand diameter and vegetation cover, as well as the influence law of the position and area of straw checkerboards on the propagation of the desertified land are analyzed.

2. Numerical model

2.1. CSCDUNE

In the model, the distribution of sand particle lift-off velocities is required as an initial condition to model macro-scale windblown sand flux; and a covering coefficient and a transportation factor matrix calculated by the probability of deposition and rebound, respectively, are employed to quantify the thickness and the transportation length of the eroded 'sand body element'. Through introducing the above statistical quantities, the different temporal and spatial scales over ranges that vary from the motion of a sand particle (that has an order of magnitude of micrometer) to the formation and evolution of a dune field (that has a magnitude of tens of kilometers) can be coupled within an integrated scheme. The model CSCDUNE contains two main parts. The first part gives the initial condition, that includes the initial values of the thickness of sand supply, wind speed of the incoming wind field, and time interval which is determined according to the real incoming wind field and thus maintains a uniform intensity in each time step. The second part describes the development process of a dune field, in which the following tasks can be achieved: 1) discretization of the sand bed; 2) calculation of the windblown sand flux for eroded 'sand body element'; 3) evaluation of the thickness and the transportation length of the eroded 'sand body element'; and 4) correction of the transportation and the relative position of the 'sand body element'. Details are briefly described as follows:

1) Discretization of the sand bed. In this case, the real local wind speed is calculated according to the significantly varying surface

configuration and the incoming wind speed. The whole field is divided into 'sand body elements' which have a thickness of $H_{n,ij}$ determined by the real local wind speed, with n as the time step, and ij denotes spatial location. The actual fictional wind velocity blowing over every single 'sand body element' is thereby deemed to be almost uniform. At the beginning of the simulations, $H_{n,ij}$ is the initial thickness of the sand bed.

2) Calculation of the windblown sand flux for the eroded 'sand body element'. The sand flux $q_{n,ij}$, the corresponding sand particles' average saltation length $\bar{l}_{n,ij}$, saltation time $\bar{t}_{n,ij}$, and the average velocities $\bar{v}_{n,ij}$ of impacting sand particles in steady-state windblown flux during ΔT_n for the eroded 'sand body element' are calculated.
3) Evaluation of the thickness and the transportation length of the eroded 'sand body element'. Firstly, the sand particles' deposition and ejection probability during ΔT_n are evaluated. Secondly, the covering coefficient and transportation factor matrix of the 'sand body element' are determined. Finally, the thickness and the transport length of the eroded 'sand body element' are calculated (see also Bo and Zheng, 2011b).
4) Correction of the transportation and the relative position of the 'sand body element'. Firstly, it is necessary to judge whether $H_{n,ij}<\eta_{n,ij}$ during ΔT_n. If so, the thickness of the eroded 'sand body element' is then set equal to$H_{n,ij}$. Secondly, an assessment is made to judge whether the 'sand body element' being moved from locations $i+1$ to $i+l_{n,ij}$ dropped into a 'protected area' where little deposition and erosion of sands happens (Frank and Kocurek, 1996; Walker and Nickling, 2002). If yes, the eroded 'sand body element' deposit at the first location of the protected area has a length ofζh, in which h is the dune height, and the coefficient is commonly taken as $\zeta=4$(Werner, 1995). If not, the transportation length of those eroded 'sand body elements' along with the wind direction is taken as$l_{n,ij}$. Thirdly, avalanche behavior is considered through moving sands at the higher position moves to the adjacent lower position when the topographic gradient of sand bed is larger than the angle of repose of the sand particle.
5) Judging whether $\sum \Delta T_n \geq T$ is satisfied. If yes, the simulation is over; if not the procedure returns to the first step and is repeated.

2.2. The simulation of dune field in desert–oasis transitional zone

The essential discrepancies between the quantitative simulation of dune fields in the desert–oasis transitional zone and that in the desert hinterland are the thickness of sand supply, inhomogeneity of vegetation cover and the non-periodicity of the boundary region introduced by the specific surface condition of the desert–oasis transitional zone. The thickness of sand supply is defined as the average height of the sand bed in the dune field which is used to describe the total volume of sands in a dune field, i.e., the product of the thickness of sand supply and the total area of a dune field equals the total volume of sands in a dune field. Therefore, in order to simulate the evolution of dune fields in the desert–oasis transitional zone, we need to make some amendments to CSCDUNE.

According to the classification of Fryberger et al. (1979), under a unidirectional wind regime, when the sand supply is sufficient, the dune field consists of transverse dunes (dune ridges with crests transverse to the dominant wind), and when the sand supply is insufficient, the dune field consists of barchans (a free transverse dune with a crescentic plan-shape in which the crescent opens downwind). Our field observations of the pattern and scale of dunes in Minqin revealed that dune patterns are dominated by large transverse dunes and chains of barchans in the desert–oasis transitional zone near the side of the Badain Jaran Desert, no sand dunes exist in the oasis, while between them there are a lot of single barchans. Therefore, we can infer that the sand supply of desert–oasis transitional zone is smaller than that of desert. To reflect the inhomogeneity of sand supply, we divided the simulation area into three kinds of areas according to the surface sand supply in CSCDUNE, the first type is the desert region, where the thickness of sand supply generally is larger than 1.1 m (Zheng et al., 2009), and the second type is the desert–oasis transition zone, where the thickness of sand supply is smaller than 1.1 m. The thickness of sand supply in the simulation of this study is assumed to be uniform, which can be given as another value according to actual distribution of sand supply for other deserts. The third area type is oasis, where the thickness of sand supply is zero, as shown in Fig. 2a.

Secondly, the field observations of Wang et al. (2007) in Minqin revealed that the wind speed changes along the desert–oasis transitional zone due to vegetation locally slowing down the wind (Durán and Herrmann, 2006), which demonstrates a continuously linear decrease along the desert–oasis transitional zone, as shown in Fig. 2b. It indicates that the simulation of dune fields in the desert–oasis transitional zone needs to consider the spatial variation of wind speed. Additional studies show that vegetation has an obvious impact on the erosion of sand particles (Buckley, 1987, 1996; Kuriyama et al., 2005; Durán and Herrmann, 2006), the windblown sand flux ratio between vegetation and no vegetation cover cases decreases exponentially with vegetation cover increasing (Buckley, 1996), i.e., $Q_n=0.95e^{-0.2\mathrm{veg}}$, where, veg represents the vegetation cover. Therefore, we made following improvements to the CSCDUNE:

1) Before calculating the change in wind speed caused by local topography, we determine the incoming wind speed $U^*(\Delta T_n, l_{\mathrm{tra}})$ at various spatial positions based on incoming wind speed $U^*(\Delta T_n)$, i.e.

$$U^*(\Delta T_n, l_{\mathrm{tra}}) = U^*(\Delta T_n)[1-c_{\mathrm{a}}(l_{\mathrm{tra}}/l_{\mathrm{sum}})] \quad (1)$$

Here, l_{tra} is the distance away from the edge of the desert, l_{sum} is the length of the desert–oasis transitional zone, ΔT_n is time step and c_a is the decreasing factor of wind speed ranging from 0.2-0.6, with a typical value of $c_{\mathrm{a}}=0.3$ in Minqin (Wang et al., 2007).
2) Considering the spatial variation of vegetation cover along the transitional zone, i.e., treating the vegetation cover veg_{ij} as the state quantity of every 'sand body element', which can be described by the following equation fitted by the results of field observations from Minqin (Jia et al., 2002), as shown in Fig. 2b,

$$\mathrm{veg} = 10\delta-36\delta^2+48\delta^3-20\delta^4 \quad (2)$$

where, $\delta=l_{\mathrm{tra}}/l_{\mathrm{sum}}$ and the *veg* is 0 and 1 for desert and oasis region, respectively. Based on this, we can calculate the actual windblown sand flux $Q_n q_{n,ij}$ of every 'sand body element', where $q_{n,ij}$ represents the windblown sand flux when *veg* is zero. It should be noted that due to the existence of vegetation, the contact area between saltating sand particles and the vegetated bed surface is less than that on the bare sand bed, which has a direct influence on the deposition probability of sand particles. The actual deposition probability of sand particles is $\left(1-\mathrm{veg}_{ij}\right)\bar{\alpha}_{ij}$, where, $\bar{\alpha}_{ij}$is the deposition probability of sand particles when veg is zero, which can be determined by $\bar{\alpha}_n = 1-0.9\left[1-e^{-2.0\times\bar{v}_n}\right]$ (Anderson and Haff, 1991), and $\bar{v}_n$ is the average impacting speed of saltating sand particles. In this study, the average saltation length and time of sand particles, as well as the average impacting speed, are assumed not to be influenced by vegetation.

For boundary conditions, it is reasonable to adopt the periodic boundary condition for the simulations of desert hinterland. However, for a desert–oasis transitional zone it has an obvious surface-property variation from desert, desert–oasis to oasis, which makes the periodic boundary condition no longer applicable. Therefore, we adopted an open boundary condition in this study, that is, when an eroded 'sand body element' leaves from the boundary of simulation area, it is not considered in the simulation.

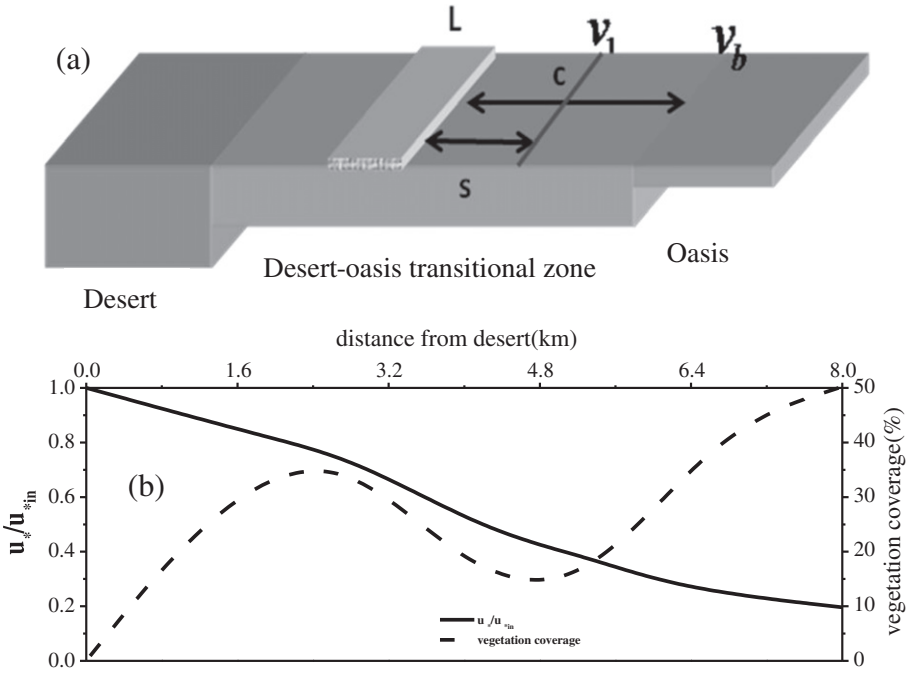

Fig. 2. Schematic diagram of the desert–oasis transitional zone (a), and the spatial variation of wind speed and vegetation cover along desert–oasis transitional zone (b).

For severe desertification, many anti-desertification measures are taken, such as establishing straw checkerboards. For example, along the edge of the Badain Jaran desert in Minqin, a large amount of straw checkerboards are set to fix sand dunes in the desert–oasis transitional zone. The existence of straw checkerboards brings special inhomogeneity of surface properties in our numerical simulations. Therefore, additional treatments are given in the simulation by CSCDUNE. Our field observations showed that the collected sand amount over a straw checkerboard-armored surface is about two orders of magnitude less than that over a bare sand surface, as shown in Fig. 3. It indicates that the existence of straw checkerboard can obviously reduce the erosion of sand particles by windblown sand flow which reduces the actual windblown sand flux to $q_{n,ij}/100$.

3. Results and discussions

Based on the numerical scheme presented in Section 2, quantitative simulations are conducted of the evolution and propagation of dune fields toward a desert–oasis transitional zone. The simulation box is 15 km in length and 4 km in width, with the length of desert, desert–oasis transitional zone and oasis set as 4.8 km, 9 km and 1.2 km respectively. The incoming frictional wind speed is 0.45 m/s, sand diameter is 0.3 mm, the thickness of sand supplies of desert and desert–oasis transitional zone are 1.1 m and 0.8 m, respectively, and the decreasing factor of wind speed is 0.3. The simulation results are shown in Fig. 4a, it can be found that the dune pattern from the desert to the oasis are changing gradually from transverse dunes, barchan chains to single barchans along with the distance from the desert to oasis, and no dune exists near the oasis, which is consistent with the field observation result obtained from Minqin, as shown in Fig. 4b–d. In addition, dunes morphology also changes from transverse dunes in the desert hinterland to the barchan chains in the desert–oasis transition zone, which indirectly show that transverse dunes are not stable, and can be decomposed into chains of barchans. This is consistent with the conclusion of Parteli et al. (2011).

At the same time, with evolution time increasing, dune scales increase but the dune number decreases, and the area occupied by dunes increases. In contrast, the dune number increases but the dune

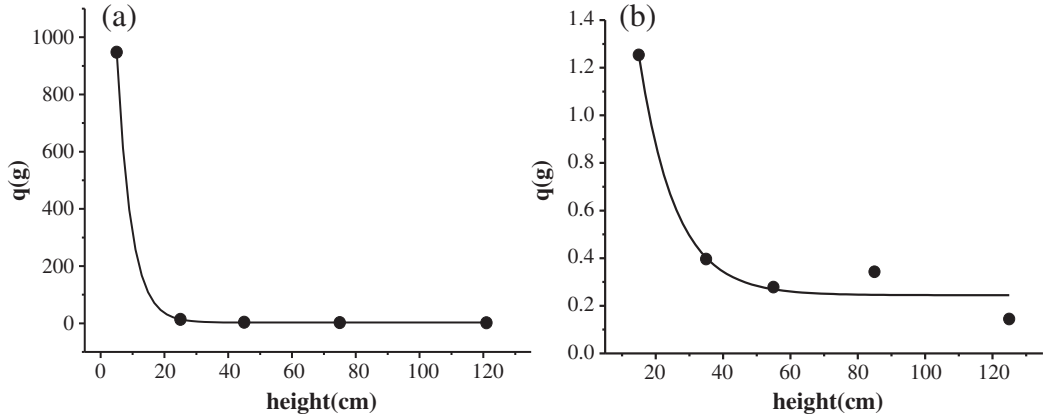

Fig. 3. Variation of collected sand amount (q) with height after sand storm over (a) sand surface and (b) straw checkerboard surface.

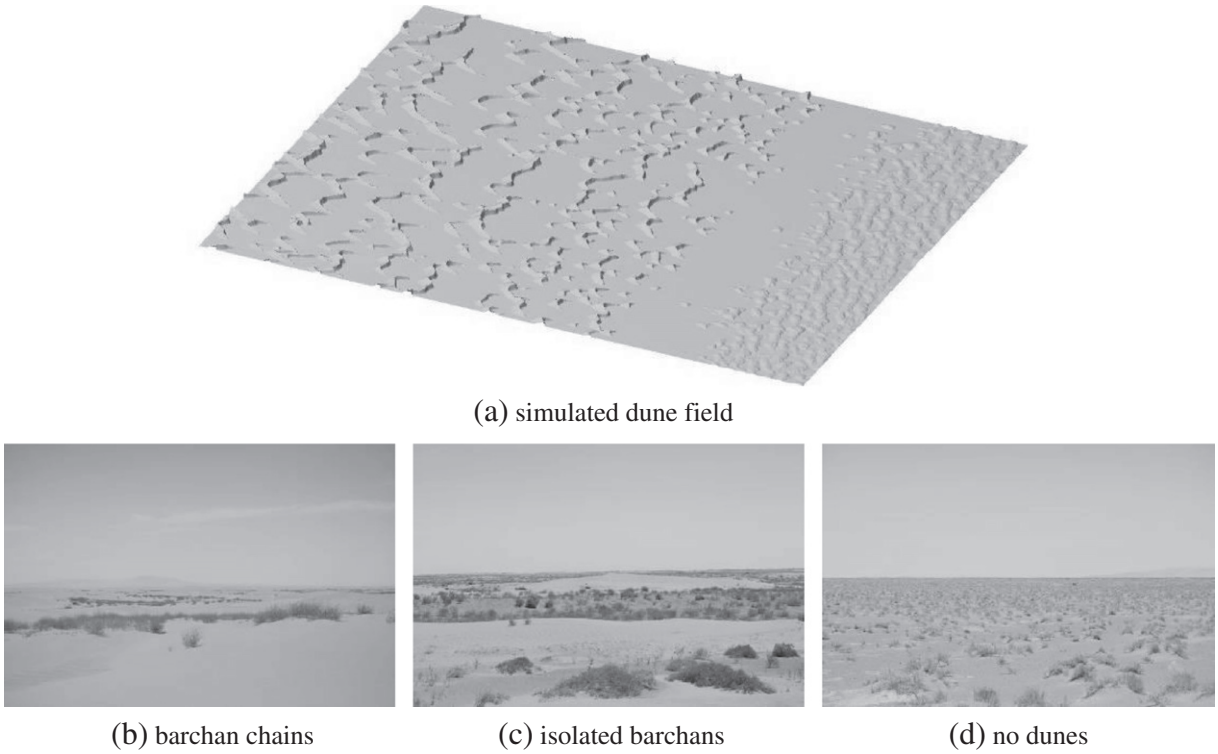

Fig. 4. Pattern of simulated dune field in desert–oasis transitional zone (a) and the actual dune pattern in the desert–oasis transitional zone of Minqin (b)–(d).

scale and the area occupied by dunes decrease with the decreasing factor of wind speed. With the incoming wind speed increasing, the dune number, dune scale and the area occupied by dunes all increase, as shown in Table 1.

In order to study the propagation speed of the edge of desert and desertified land, we firstly simulate the evolution process of dune fields in the desert–oasis transitional zone, lasting for 25 years based on above method, and then continue simulating the evolution process of dune field with the initial pattern taken as the first 25 years' patterns and the thickness of sand supply of the studied location as zero. The propagation speed is determined by the ratio between the moving distance of the position where thickness of sand supply is larger than 0.5 m close to the oasis and time *T*. Simulation results are demonstrated in Figs. 5 and 6. From Fig. 5a we can see that the propagation speed of the edge of desert increases linearly with increasing wind speed. In order to validate the model, we performed field observations on the propagation speed of the edge of desert using Magellan high-precision global positioning system, our observational results show that the propagation speed of the desert edge is about 11.2 m/yr for a sand diameter of 0.3 mm and the average wind strength and prevailing direction are 0.45 m/s and northwest, respectively. The distribution of wind strength and wind rose are given in Fig. 7. Given the same sand diameter and wind power conditions, the simulated propagation speed by our model is about 11.0 m/yr, which is close to the field observation results in quantity, and the relative error between field observation results and simulation result is smaller than 2%. Fig. 5b shows that when sand diameter is larger than 0.3 mm or smaller than 0.25 mm, with increasing sand diameter the propagation speed of the desert edge decreases linearly; when sand diameter is larger than 0.25 mm and smaller than 0.3 mm, the propagation speed of desert edge does not change significantly. At the same time, from Fig. 5a we can see that when frictional wind speed is larger than 0.43 m/s, the edge of desertified land begins to propagate and the propagation speed increase exponentially with wind speed. When sand diameter is larger than 0.3 mm or smaller than 0.25 mm, with increasing sand diameter the propagation speed of desertified land decreases linearly; and when sand diameter is larger than 0.25 mm and smaller than 0.3 mm, the propagation speed of desertified land does not change significantly.

From Fig. 6a we can see that when the distance from the edge of desert is smaller than 2 km, the propagation speed of desertified land decreases linearly with increasing distance; when the distance is larger than 2 km and smaller than 5 km, with increasing distance the propagation speed does not change significantly; and when the distance is larger than 5 km, the propagation speed decreases linearly with increasing distance. The variation of propagation speed of desertified land with a deceasing factor of wind speed is given in Fig. 6b, it shows that the propagation speed decreases with the decreasing factor of wind speed in a negative exponential way.

Actually the propagation speed of desertified land at different location of the desert–oasis transitional zone is related to local wind speed and vegetation cover. For further study of the relationship between propagation speed of desertified land and the above factors, we analyzed the variation law of propagation speed with local wind speed and vegetation cover in detail, the results of which are shown in Fig. 8. It demonstrates that when local wind speed is kept constant, with increasing vegetation cover the propagation speed of desertified land decreases in a negative exponential way; when vegetation cover

Table 1
Variation of the dune scale, dune number and the area occupied by dunes in the desert–oasis transitional zone with evolution time, decreasing factor of wind speed and incoming wind speed.

	Dune scale	Dune number	Area occupied by dunes
Evolution time	increase	decrease	increase
Decreasing factor of wind speed	decrease	increase	decrease
Incoming wind speed	increase	increase	increase

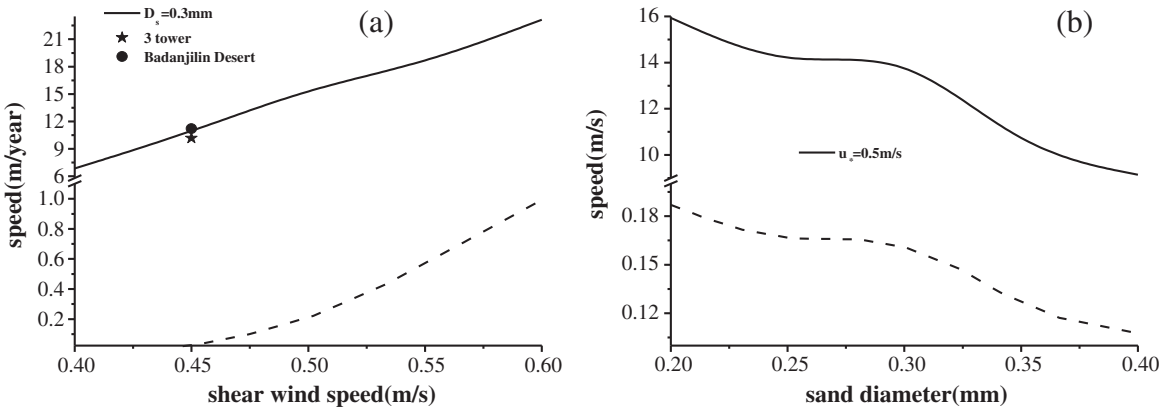

Fig. 5. Propagation speed of the edge of desert and desertified land with wind speed (a) and sand diameter (b) (solid line and dash line are the propagation speed of the edge of desert and desertified land respectively).

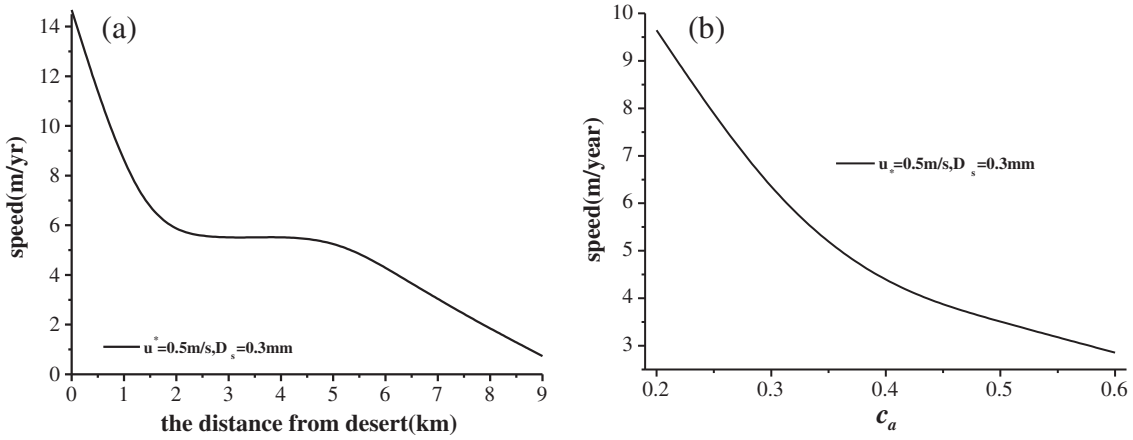

Fig. 6. Variation of propagation speed of desertified land along the desert–oasis transitional zone (a), and the variation of propagation speed of desertified land with the decreasing factor of wind speed, the distance from the edge of desert is 3 km (b).

remains invariant, with increasing local wind speed the propagation speed of desertified land increases linearly. Consequently, the propagation speed of the desertified land with respect to vegetation cover and local wind speed can be described by the following formula:

$$v_d = 8u_* - 3 + (98u_* - 28)e^{-veg} \quad (3)$$

where, u^* is the local wind speed, which is a function of locations in the desert–oasis transitional zone as indicated in Eq. (1).

Based on Eq. (3), we can predict the propagation speed of desertified land by simply measuring the local wind speed u^* and the value of veg; it can also obtain the threshold value of wind speed for various vegetation cover conditions when the propagation speed is equal to zero.

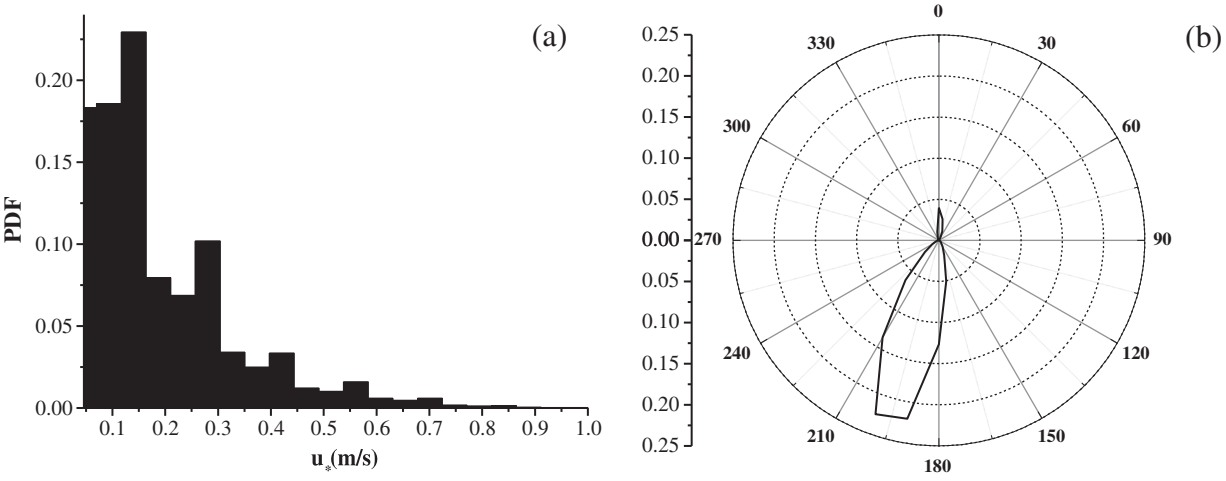

Fig. 7. Distribution of wind strength (a) and wind rose when the wind speed is over the threshold wind speed of Minqin in 2009.

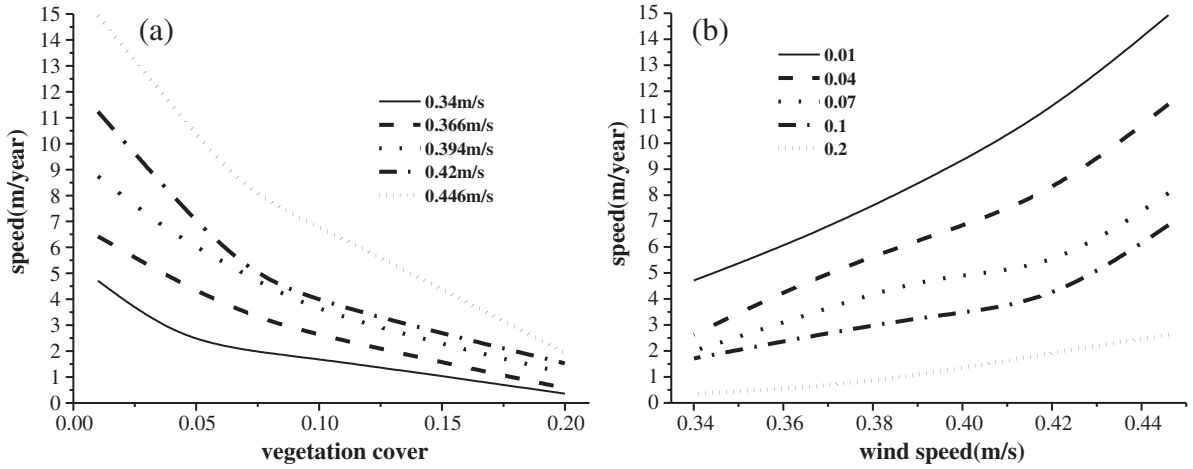

Fig. 8. Variation of propagation speed of desertified land with vegetation cover (a) and local wind speed (b).

When the local wind speed is smaller than the threshold value, the desertified land does not propagate, otherwise the desertified land propagates. Furthermore, we can obtain the values of local wind speed and vegetation cover corresponding to different propagation speeds, as shown in Fig. 9a. According to this relationship, the propagation speed can be controlled by adjusting vegetation cover based on the local wind speed of different position, for example, when the local wind speed is 0.5 m/s, the vegetation cover of the bed surface must larger than 0.4 so as to make the propagation speed smaller than 1 m/year. Moreover, our results show that the threshold wind speed above which the edge of desert starts to propagate increases with vegetation cover. It is consistent with the conclusion of Yizhaq et al. (2007) in quality.

In addition, we can analyze the variation of propagation speed of desertified land after laying straw checkerboards. The results show that the desertified land with straw checkerboards does not propagate, which indicates that these checkerboards can fix sand dune very well. More specifically, at the upwind side of the area with straw checkerboards, the propagation speed of desertified land has not obviously change, but the propagation speed of desertified land at the downwind side is affected by straw checkerboards. Taking the propagation speed of the edge of desertified land (v_b) for example, as shown in Fig. 9b, the propagation speed of the edge of desertified land with straw checkerboards is less than that without. Further the influence of incoming wind speed, the length L of straw checkerboard area, and the distance c between the straw checkerboard area and the edge of desertified land on the reduction rate of propagation speed of the edge of desertified land are shown in Fig. 8, in which the reduction rate is defined as $1-v/v_{no}$, here, v is the propagation speed of the edge of desertified land with straw checkerboards, v_{no} is the propagation speed of the edge of desertified land without straw checkerboards. From Fig. 10 we can see that when c is less than 800 m, with increasing c the reduction rate of propagation speed of the edge of desertified land decreases gradually; when c is larger than 800 m, with increasing c the reduction rate decreases rapidly. At same time, from figure we can also find that the reduction rate decreases linearly with increasing wind speed. When L is less than 400 m, with increasing L the reduction rate increases; when L is larger than 400 m, the reduction rate does not change obviously with increasing L, as shown in Fig. 11.

4. Conclusion

Quantitative simulations of dune fields in the desert–oasis transitional zone were achieved by considering the spatial variation of wind speed, the influence of vegetation on sand erosion and transportation, etc. The variation law of propagation speed at the edge of desert and desertified land was also analyzed, as well as the influence of a straw checkerboard area on the propagation speed. The results show that the dominating dune pattern includes transverse dunes,

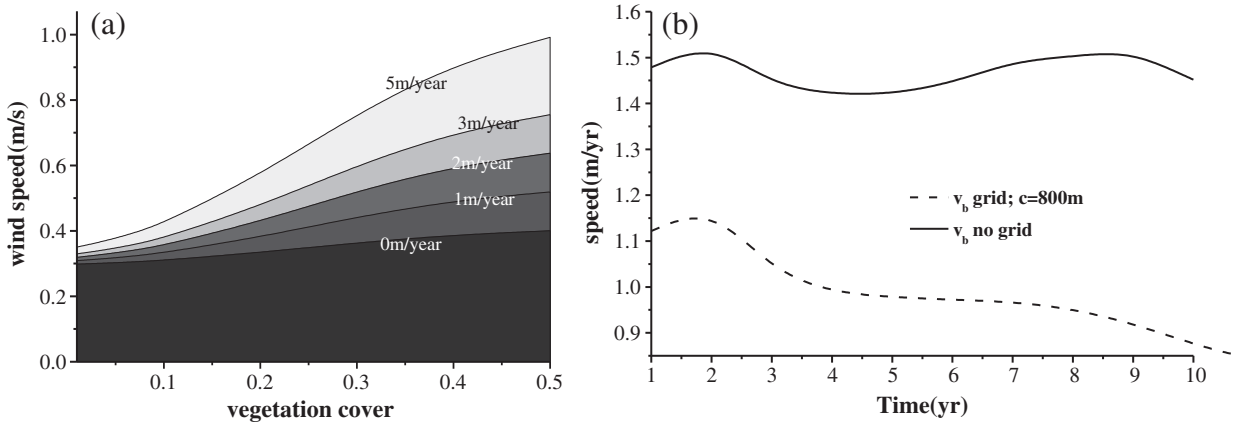

Fig. 9. Phase diagram of propagation speed of desertified land (a) and the propagation speed of the edge of desertified land varies with evolution time (b), where, v_b is the propagation speed of the edge of desertified land and $c=800$ m is the distance between the straw checkerboard area and the edge of the desertified land.

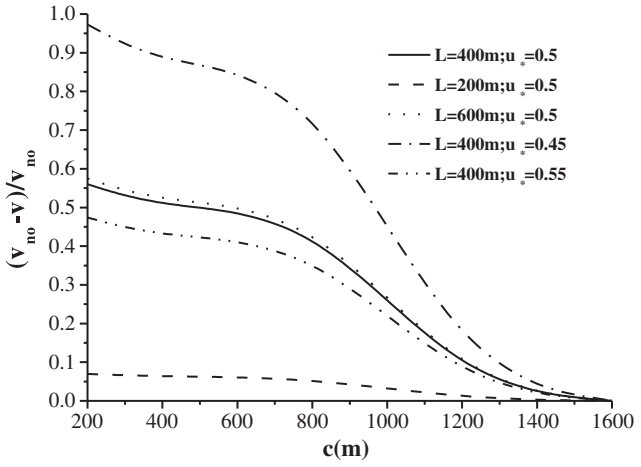

Fig. 10. Propagation speed of the edge of desertified land varies with c, where c is the distance between the straw checkerboard area and the edge of desertified land, v is the propagation speed of the edge of desertified land with straw checkerboards, v_{no} is the propagation speed of the edge of desertified land without straw checkerboards, and L is the length of straw checkerboard area.

barchan chains and barchans, respectively, from desert to oasis, and no dune exists in the oasis. The dune scale, dune number and the area occupied by dunes in a desert–oasis transitional zone change with evolution time, decreasing factor of wind speed and incoming wind speed. The propagation speed of the edge of desertified land is related to the incoming wind speed, sand diameter, the deceasing factor of wind speed and locations. In fact, local wind speed and vegetation cover play prominent role, i.e., the propagation speed of desertified land decreases negatively exponentially and increases linearly with vegetation cover and local wind speed, respectively, which can be described by Eq. (3).

In terms of the effects of straw checkerboards, the propagation speed of desertified land at the downwind area decreases with the emplacement of a straw checkerboard, i.e. with increasing c the reduction rate of propagation speed of the edge of desertified land decreases, when L is less than 400 m, with increasing L the reduction rate increases; when L is larger than 400 m the reduction rate does not change obviously with increasing L. This implies that it is not necessary to lay straw checkerboards continuously over the sand bed surface in a sand-control engineering project, for example, the length L of the straw checkerboard area can be 400 m and the interval between straw checkerboards can be 800 m.

Acknowledgements

This research was supported by a grant from the National Natural Science Foundation of China (no. 11072097, no. 11232006, no. 11202088), the Science Foundation of Ministry of Education of China (no. 308022), Fundamental Research Funds for the Central Universities (lzujbky-2009-k01), the National Key Technology R&D Program (No. 2009BAC53B01) and the Project of the Ministry of Science and Technology of China (no. 2009CB421304). The authors express their sincere appreciation to the supports.

References

Aidun, J.B., Lo, D.C.S., Trucano, T.G., Fye, R.M., 1999. Representative Volume Size: a Comparison of Statistical Continuum Mechanics and Statistical Physics. Technical report, Sandia National Laboratories, New Mexico.
Anderson, R.S., Haff, P.K., 1991. Wind modification and bed response during saltation of sand in air. Acta Mechanics (Suppl. 1), 21–51.
Anthonsen, K., Clemmensen, L., Jensen, J., 1996. Evolution of a dune from crescentic to parabolic form in response to short-term climatic changes: Råbjerg Mile, Skagen Odde, Denmark. Geomorphology 17, 63–77.
Bo, T.L., Zheng, X.J., 2011a. The formation and evolution of aeolian dune fields under unidirectional wind. Geomorphology 134, 408–416.
Bo, T.L., Zheng, X.J., 2011b. Bulk transportation of sand particles in quantitative simulations of dune field evolution. Powder Technology 214, 243–251.
Buckley, R., 1987. The effect of sparse vegetation on the transport of dune sand by wind. Nature 325, 426–428.
Buckley, R., 1996. Effects of vegetation on the transport of dune sand. Annals of Arid Zone 35 (3), 215–223.
Chen, L.D., Liu, Y., Lu, Y.H., Feng, X., Fu, B., 2008. Pattern analysis in landscape ecology: progress, challenges and outlook. Acta Ecologica Sinica 28 (11), 5521–5531.
Durán, O., Herrmann, H.J., 2006. Vegetation against dune mobility. Physical Review Letters 97, 188001.
Durán, O., Silva, M., Bezerra, L., Herrmann, H., Maia, L., 2008. Measurements and numerical simulations of the degree of activity and vegetation cover on parabolic dunes in northeastern Brazil. Geomorphology 102, 460–471.
Frank, A., Kocurek, G., 1996. Airflow up the stoss slope of sand dunes: limitations of current understanding. Geomorphology 17, 47–54.
Fryberger, S.G., Dean, G., McKee, E.D., 1979. Dune forms and wind regime. In: McKee, E.D. (Ed.), A Study of Global Sand Seas. : Professional Paper, 1052. US Geological Survey, Denver, pp. 137–170.
Fu, B.J., Lu, Y.H., 2006. The progress and perspectives of landscape ecology in China. Progress in Physical Geography 30, 232–244.
Gaylord, D., Stetler, L., 1994. Aeolian-climatic thresholds and sand dunes at the Hanford Site, south-central Washington, U.S.A. Journal of Arid Environments 28, 95–116.
Hack, J., 1941. Dunes of the western Navajo country. Geography Review 31 (2), 240–263.
Jia, B.Q., Ci, L.J., Cai, T.J., Gao, Z.H., Ding, F., 2002. Preliminary research on environmental characteristics of oasis–desert ecotone. Chinese Journal of Applied Ecology 13 (9), 1104–1108.
Kuriyama, Y., Mochizuki, N., Nakashima, T., 2005. Influence of vegetation on aeolian sand transport rate from a backshore to a foredune at Hasaki, Japan. Sedimentology 52 (5), 1123–1132.
Li, X., Lu, L., Cheng, G.D., Xiao, H.L., 2001. Quantifying landscape structure of the Heihe River Basin, northwest China using FRAGSTATS. Journal of Arid Environments 48 (4), 521–535.

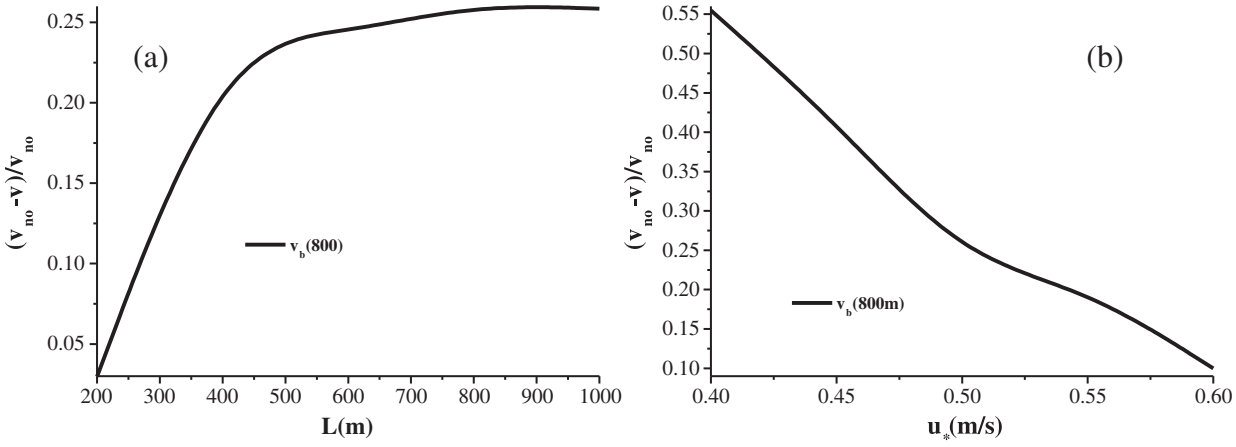

Fig. 11. Reduction rate of propagation speed of the edge of desertified land varies with L (a) and incoming wind speed (b), where, v_b is the propagation speed of the edge of desertified land, $c = 800$ m is the distance between the straw checkerboard area and the edge of desertified land, v is the propagation speed of the edge of desertified land with straw checkerboards, v_{no} is the propagation speed of the edge of desertified land without straw checkerboards, and L is the length of straw checkerboard area.

Luna, M.C.M.M., Parteli, E.J.R., Durán, O., Herrmann, H.J., 2009. Modeling transverse dunes with vegetation. Physica A: Statistical Mechanics and its Applications 388, 4205–4217.
Luna, M.C.M.M., Parteli, E.J.R., Durán, O., Herrmann, H.J., 2011. Model for the genesis of coastal dune fields with vegetation. Geomorphology 129, 215–224.
Momiji, H., Carretero-GonzÃalez, R., Bishop, S.R., Warren, A., 2000. Simulation of the effect of wind speedup in the formation of transverse dune fields. Earth Surface Processes and Landforms 25, 905–918.
Muckersie, C., Shepherd, M., 1995. Dune phases as time-transgressive phenomena, Manawatu, New Zealand. Quaternary International 26, 61–67.
Narteau, C., Zhang, D., Rozier, O., Claudin, P., 2009. Setting the length and time scales of a cellular automaton dune model from the analysis of superimposed bed forms. Journal of Geophysical Research 114, F03006.
Nield, J.M., Baas, A.C.W., 2008. The influence of different environmental and climatic conditions on vegetated aeolian dune landscape development and response. Global and Planetary Change 64 (1–2), 76–92.
Nishimori, H., Ouchi, H., 1993. Formation of Ripple Patterns and Dunes by Wind-Blown Sand. Physical Review Letters 71, 197–200.
Nishimori, H., Tanaka, H., 2001. A simple model for the formation of vegetated dunes. Earth Surface Processes and Landforms 26, 1143–1150.
Parteli, E.J.R., Durán, O., Herrmann, H.J., 2007. Minimal size of a barchan dune. Physical Review E 75, 011301.
Parteli, E.J.R., Andrade, J.S., Herrmann, H.J., 2011. Transverse instability of dunes. Physical Review Letters 107, 18801.
Reitz, M.D., Jerolmack, D.J., Martin, R.L., Ewing, R.C., 2010. Barchan–parabolic dune pattern transition from vegetation stability threshold. Geophysical Research Letters 37, L19402.
Rubin, D., Hunter, R., 1987. Bedform alignment in directionally varying flows. Science 237, 276–278.
Sauermann, G., Kroy, K., Herrmann, H.J., 2001. A continuum saltation model for sand dunes. Physical Review E 64, 31305.
Schwammle, V., Herrmann, H.J., 2003. Solitary wave behaviour of dunes. Nature 426, 619–620.
Thomas, D.S.G., Knight, M., Wiggs, G.F.S., 2005. Remobilization of southern African desert dune systems by twenty-first century global warming. Nature 435, 1218–1221.
Tsoar, H., Blumberg, D., 2002. Formation of parabolic dunes from barchan and transverse dunes along Israel's Mediterranean coast. Earth Surface Processes and Landforms 27, 1147–1161.
Walker, I.J., Nickling, W.G., 2002. Dynamics of secondary airflow and sediment transport over and in the lee of transverse dunes. Progress in Physical Geography 26, 47–75.
Wang, B., Cui, X.H., 2004. Researches on laws of water balance at transitional zone between oasis and desert in Minqin. Acta Ecologica Sinica 24 (2), 235–240.
Wang, J.Y., Jiang, Z.R., Wang, J.H., Zhang, D.H., 2006. Natural vegetation characteristic of three sand dune types in the Minqin oasis–desert ecotone. Journal of Gansu Agricultural University 41 (2), 51–55.
Wang, S.T., Zou, X.Y., Zhang, C.L., Cheng, H., 2007. Wind-protecting effect of shrub dunes in ecotone of Minqin oasis. Scientia Geographica Sinica 27 (1), 104–108.
Wasson, R.J., Hyde, R., 1983. Factors determining desert dune type. Nature 304, 337–339.
Werner, B.T., 1995. Eolian dunes: computer simulations and attractor interpretation. Geology 23, 1107–1110.
Wolfe, S., Hugenholtz, C., 2009. Barchan dunes stabilized under recent climate warming on the northern Great Plains. Geology 37, 1039–1042.
Yizhaq, H., Ashkenazy, Y., Tsoar, H., 2007. Why do active and stabilized dunes coexist under the same climatic conditions? Physical Review Letters 98 (18), 188001.
Yizhaq, H., Ashkenazy, Y., Tsoar, H., 2009. Sand dune dynamics and climate change: a modeling approach. Journal of Geophysical Research 114, F01023.
Zheng, X.J., 2009. Mechanics of Wind-blown Sand Movement. Springer, German.
Zheng, X.J., Bo, T.L., Zhu, W., 2009. A scale-coupled method for simulation of the formation and evolution of aeolian dune field. International Journal of Nonlinear Sciences & Numerical Simulation 10 (3), 387–395.